JCTC Journal of Chemical Theory and Computation

TD-DFT Performance for the Visible Absorption Spectra of Organic Dyes: Conventional versus Long-Range Hybrids

Denis Jacquemin,*[,†] Eric A. Perpète,[†] Gustavo E. Scuseria,[‡] Ilaria Ciofini,[§] and Carlo Adamo*[,§]

Laboratoire de Chimie Théorique Appliquée, Groupe de Chimie-Physique Théorique et Structurale, Facultés Universitaires Notre-Dame de la Paix, rue de Bruxelles, 61, B-5000 Namur, Belgium, Department of Chemistry, Rice University, Houston, Texas 77005, and Ecole Nationale Supérieure de Chimie de Paris, Laboratoire Electrochimie et Chimie Analytique, UMR CNRS-ENSCP no. 7575, 11, rue Pierre et Marie Curie, F-75321 Paris Cedex 05, France

Abstract: The $\pi \rightarrow \pi^*$ transitions of more than 100 organic dyes from the major classes of chromophores (quinones, diazo, ...) have been investigated using a Time-Dependent Density Functional Theory (TD-DFT) procedure relying on large atomic basis sets and the systematic modeling of solvent effects. These calculations have been performed with pure (PBE) as well as conventional (PBE0) and long-range (LR) corrected hybrid functionals (LC-PBE, LC-ωPBE, and CAM-B3LYP). The computed wavelengths are systematically guided by the percentage of exact exchange included at intermediate interelectronic distance, i.e., the λ_{max} value always follows the PBE > PBE0 > CAM-B3LYP > LC-PBE > LC-ωPBE > HF sequence. The functional giving the best estimates of the experimental transition energies may vary, but PBE0 and CAM-B3LYP tend to outperform all other approaches. The latter functional is shown to be especially adequate to treat molecules with delocalized excited states. The mean absolute error provided by PBE0 is 22 nm (0.14 eV) with no deviation exceeding 100 nm (0.50 eV): PBE0 is able to deliver reasonable estimates of the color of most organic dyes of practical or industrial interest. By using a calibration curve, we found that the LR functionals systematically allow an even more consistent description of the low-lying excited-state energies than the conventional hybrids. Indeed, linearly corrected LR approaches yield an average error of 10 nm for each dye family. Therefore, when such statistical treatments can be designed for given sets of dyes, a simple and rapid theoretical procedure allows both a chemically sound and a numerically accurate description of the absorption wavelengths.

I. Introduction

Though dyes could be classified with respect to the chemical process generating the color (absorption/fluorescence/ phosphorescence) or to the nature of the implied excited states ($\pi \rightarrow \pi^*/n \rightarrow \pi^*$), one generally groups them according to the nature of their chromophoric unit (Figure 1).[1−3] The two major families of organic dyes with industrial applications are 9,10-anthraquinones (AQ) and azobenzenes (AB), that represents about 30% and 60% of today's world dye production, respectively.[1−3] The longest wavelength of maximal absorption (λ_{max}) of AQ covers all the visible region of the electromagnetic spectrum, depending on the nature

* Corresponding author e-mail: denis.jacquemin@fundp.ac.be, http://perso.fundp.ac.be/~jacquemd (D.J.), carlo-adamo@enscp.fr (C.A.).
† Facultés Universitaires Notre-Dame de la Paix.
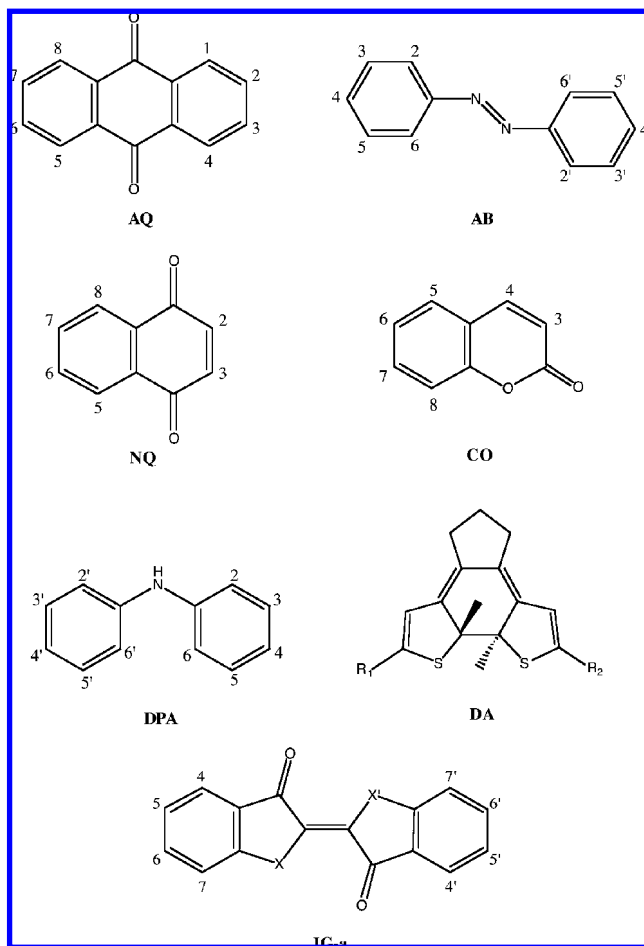‡ Rice University.
§ UMR CNRS-ENSCP no. 7575.

Figure 1. Sketch of the chromophores investigated in this study.

Figure 2. Studied indigoids derivatives.

and position of the auxochromic group(s) substituting positions 1-to-8.[2,4] AB are extremely versatile,[3] with applications going from core of media storages,[5] to central building blocks in molecular motors.[6,7] Of course, several other chromophores related to more specific applications can be pinpointed: (1) naphthoquinones (NQ), implied in several medicinal processes;[8,9] (2) coumarins (CO), the most efficient fluorescent brighteners;[10] (3) diphenylamine derivatives (DPA), the typical hair dyes with important biological properties;[11,12] (4) diarylethenes (DA), the prototype molecular switch;[13−15] and (5) indigoids derivatives (IG, Figure 2) which give loads of structures with several substitution patterns of the outer phenyl rings, of the heteroatoms, as well as different types of linkage between the two parts of the molecule.[3] Developing molecular modelization approaches allowing an accurate prediction of the color of dyes is still a major challenge,[16] because, on the one hand, the average human eye is able to tell apart shades differing by 1 nm only, and, on the other hand, actual stains are medium-sized molecules, possess a dozen π-electrons, and are very sensitive to the environments. Therefore, large-scale highly correlated ab initio approaches such as EOM-CC, MR-CI, or CAS-PT2 remain out of today's computational reach. Consequently, one could be inclined to select customized semiempirical approaches such as ZINDO, but the consistency of such schemes is often disappointing.[17−19] Currently, the most widely applied ab
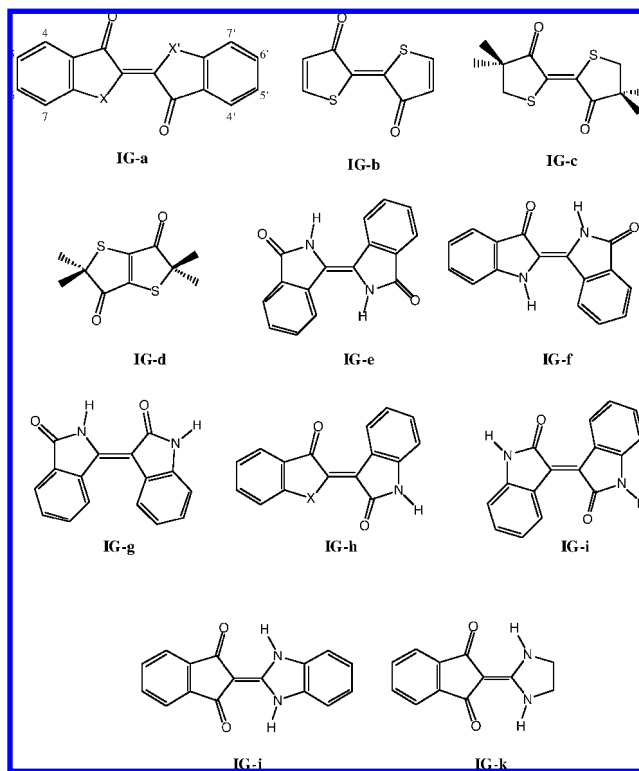
initio tool for modeling electronic spectra of structures is the time-dependent density functional theory (TD-DFT).[20] TD-DFT calculations can incorporate environmental effects[21] and quickly give UV/vis spectra for most organic[22−25] and inorganic[26,27] dyes. Still, meaningful results can only be attained with a selection of adequate exchange-correlation functionals. It is recognized that conclusions obtained with hybrid functionals tend to be in better agreement with experimental trends than the values computed with pure functionals. Hybrids, originally proposed in the 1990s,[28,29] include a fraction (α) of *exact* exchange that is computed with the Hartree−Fock (HF) exchange formula.[28−40] Despite their countless successes, hybrids also encounter problems that seem (mostly) independent of the functional selected. Typical troublesome properties include van der Waals forces,[41] bond length alternation (BLA) in semiconducting polymers,[42,43] nonlinear optics (NLO) properties of long π-conjugated chains,[44,45] and charge-transfer electronic transitions.[17,46−49] In these four cases, no single α value provides a small (or consistent) error for increasingly large/spaced compounds. In fact, these DFT limitations have a common origin: the so-called shortsightedness of DFT functionals. In other words, the density is not influenced by a change in the nearby electronic distribution.[44,47,48] To circumvent these shortcomings, several strategies have been designed and applied to the problems listed above: the correction(s) of the self-interaction error,[50−52] the inclusion of the current-density in the formalism,[53,54] the addition of empirical dispersion terms,[55,56] and the use of optimized effective potential for exact exchange[57,58] as well as the explicit consideration of long-range effects (LR).[59−86] This latter scheme leads to the *range-separated* hybrids that use a growing fraction of exact exchange when the interelectronic

TD-DFT Performance for the Spectra of Organic Dyes

J. Chem. Theory Comput., Vol. 4, No. 1, 2008 **125**

distance increases (see section II). In contrast, the hybrids in which the amount of HF exchange is constant all over the space will be referred to as *global* hybrids in the following (*conventional* or *full-range exchange* hybrids have also been used in the literature). It has been demonstrated that range-separated hybrids are very efficient for calculating BLA[82] or NLO[61,67,68,82,83,87] properties in conjugated polymers as well as for determining properties of weakly bond complexes[64,70,85] or charge-transfer states in large molecular systems.[64,68,74−77,81] Nevertheless, there have been only a few works establishing the abilities of TD-LR-DFT to reproduce experimental UV/vis spectra for a statistically meaningful set of compounds: (1) comparisons of global and range-separated functionals performances for the vertical transitions of C=O, N_2, C_2H_4, H_2O, C_6H_6, and H_2C=O demonstrated that, while Rydberg's states are much better described with the latter, differences remain small for valence excited states;[64,73,85] (2) the emission properties of low-lying excited-states of small molecules have also been investigated, and similar conclusions have been drawn;[74] (3) we have studied the localized $n \rightarrow \pi^*$ transitions in nitroso and thiocarbonyl dyes, and it turned out that all hybrid functionals lead to a quite similar accuracy;[88] (4) the λ_{max} of four CO dyes are more accurate with global TD-DFT than with (unmodified) TD-LR-DFT;[84] (5) for the $\pi \rightarrow \pi^*$ transitions of 15 AQ, it has been found that range-separated hybrids are further away from experimental values than their global counterparts but offer a much smaller statistical dispersion of the results, allowing more valid chemical insights;[82] and (6) on the contrary, TD-LR-DFT brings no significant correction for cyanine derivatives, as these dyes present a strong multide-terminantal nature.[82]

In this paper, we perform a critical assessment of the efficiency and consistency of range-separated hybrids for computing the main $\pi \rightarrow \pi^*$ transition of industrial organic dyes. The generic chromophores we have considered are depicted in Figure 1. It is worth pointing out previous TD-DFT investigations for these compounds. For AQ, the performance of global hybrids has been assessed in refs 19, 22, 46, and 89−93, while our previous work used TD-LR-DFT.[82] Numerous computations of the UV/Visible spectra of AB based on TD-DFT have been published,[46,94−98] but to our best knowledge none used range-separated hybrids. NQ, DPA, and IG have recently been tackled by two of us in refs 99, 100, 101, and 102−105, respectively. For CO, one finds several investigations performed with global hybrids,[106−113] but only one used range-separated functionals and was limited to four molecules.[84] The transition spectra of the photochromic DA switches have also been thoroughly investigated, though only with global hybrids.[15,18,114−123] In fact, the molecules in Figures 1 and 2 include most of the families selected by Guillaumont and Nakamura[46] (we excluded cyanine-like dyes that present a multideterminental nature) but with (much) more structures in each subset.

This paper is organized as follows. In section II, we briefly summarize our computational approach. In section IIIA, the spectra of the various families computed with several pure, global, and range-separated hybrids are compared to experimental data. In section IIIB, we examine the possibilities of

statistical treatment of the theoretical λ_{max}, before concluding in section IV.

II. Methodology

In range-separated functionals, the Coulomb operator is partitioned as[59,60,63,65]

$$\frac{1}{r_{12}} = \frac{1 - [\alpha + \beta \, \text{erf}(\omega r_{12})]}{r_{12}} + \frac{\alpha + \beta \, \text{erf}(\omega r_{12})}{r_{12}} \quad (1)$$

where ω is the range separation parameter, while α and $\alpha + \beta$ define the exact exchange percentage at $r_{12} = 0$ and $r_{12} = \infty$, respectively. In eq 1, $0 \leq \alpha + \beta \leq 1$, $0 \leq \alpha \leq 1$, and $0 \leq \beta \leq 1$, are three conditions to be satisfied. Equation 1 leads to the partitioning of the total exchange energy into short-range and long-range contributions:

$$E_x = E_x^{sr} + E_x^{lr} \quad (2)$$

In this paper, three range-separated functionals have been used: (1) the LC (LC: long-range correction) scheme of Hirao[61] applied to the PBE functional,[124] (2) the LC-ωPBE functional by Vydrov and Scuseria,[77] and (3) Handy's CAM-B3LYP (CAM-B3LYP: Coulomb-attenuating method applied to B3LYP).[65] Both LC models use $\alpha = 0$ and $\beta = 1$ in eq 1, i.e. short-range semilocal DFT exchange is combined with long-range HF exchange integrals. Since $\alpha + \beta = 1$, the exchange potential in LC functionals has the exact asymptotic behavior. Note that in LC-ωPBE, the short-range exchange functional can be rigorously derived[62,125] by integration of the model exchange hole.[77,78] In CAM-B3LYP, $\alpha = 0.19$ and $\beta = 0.46$ are plugged in, and the exact asymptote of the exchange potential is lost, while a larger percentage of HF exchange is included at short range. The range separation parameter, ω in LC-PBE and CAM-B3LYP, is set to the standard 0.33 bohr^{-1} value, whereas for LC-ωPBE, we use the optimized 0.40 bohr^{-1} value from refs 77 and 78. Recently, such 0.40 bohr^{-1} value has been advocated by Fromager and co-workers,[86] whereas Hirao et al. proposed a reoptimized value of 0.47 bohr^{-1} for reaction barriers.[126] As our goal is to assess the merits of range-separated and global hybrids for visible spectra simulations, we have also performed time-dependent calculations with a pure functional (PBE),[124] a global hybrid (PBE0, that contains 25% of exact exchange),[33,34] and the HF approach (in this paper HF results are obtained through the TD-HF approach). Readers interested in the results of other global hybrids, such as the archetype B3LYP, are refered to 89 for AQ, 109 for CO, and 105 for IG. The evolution with r_{12} of the exact exchange percentage used in the six considered models is sketched in Figure 3All calculations have been performed with the Gaussian03 suite of programs,[127] except for the LR-DFT calculations that were carried out with a development version of Gaussian,[128] using their standard TD-DFT procedure (ref 129). For each system, the ground-state structure has been determined by a standard force-minimization process, and the vibrational spectrum has been determined to systematically check that all vibrational frequencies are real. All these ground-state calculations have been performed with PBE0 using a triple-ζ polarized basis set, 6-311G(d,p), that
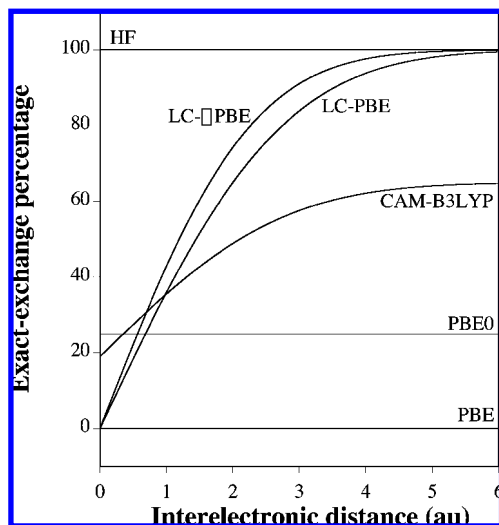
Figure 3. Evolution of the percentage of exact exchange included as the function of the interelectronic distance for the six models considered.

is known for providing converged ground-state structural parameters for the largest majority of the compounds.[130−132] In previous investigations, we have demonstrated that PBE0/6-311G(d,p) geometries are perfectly adequate for most classes of organic dyes investigated here,[18,99,101−105,122] and we refer the interested readers to these publications for discussion of the basis set effects. TD-DFT is then used to compute the three-to-eight first low-lying excited states of each dye. The resulting electronic excitations have a strong $\pi \rightarrow \pi^*$ character associated with a large oscillator force. We have systematically selected the 6-311+G(2d,p) basis set for these TD-DFT calculations, as it yields perfectly converged λ_{max} for IG,[102,103] DPA,[101] NQ,[99] and DA[18,122] dyes. For AQ, a smaller basis set would even be enough to attain the saturation of transition energies.[89,90] Therefore, we are very confident that all results presented here would not have been significantly affected by a further extension of the basis sets. At each step, the surrounding effects have been included by means of the Polarizable Continuum Model,[133] as valuable theory/experiment comparisons indeed require simulation of the solvent. Two models have been used the default IEF-PCM and the conducting PCM model (C-PCM). Computational details might slightly vary from one dye family to another (radii used to build the cavity, use of smoothing spheres, etc.) because we have set these computational parameters in order to maintain consistency with previously published data. Nevertheless, this should have a completely negligible impact on the computed wavelengths.[101] In this paper, we have selected the so-called nonequilibrium procedure for TD-DFT calculations, that has been specifically designed for the study of absorption processes.[21]

In many cases, several experimental values are available, and the values reported in Tables 1−5 correspond to the average measure. The selection of the theoretical wavelength is often straightforward: it is the first transition with a significant oscillator force.[19,99−105,110,123] In fact, to perfectly simulate experimental results, the main missing components are the vibronic couplings. Indeed, in some cases, the inclusion of Franck−Condon factors could be essential to

get the best theory/experiment match.[113] However, a systematic computation of such vibronic effects is not practically feasible for our very extended set.

III. Results

A. Comparisons with Experiments. The λ_{max} computed for 24 typical AQ dyes are reported in Table 1. For all compounds, the absorption wavelengths systematically obey: PBE > PBE0 > CAM-B3LYP > LC-PBE > LC-ωPBE > HF. This means that the larger the exact exchange ratio at intermediate r_{12} (see Figure 3), the smaller the calculated λ_{max}. For nitroso and thiocarbonyl compounds, such a systematic relationship could not be unravelled,[88] probably due to the more localized nature of the transition in these $n \rightarrow \pi^*$ chromophores: the mixing percentage at smaller distances had a larger influence. Consistently with our previous studies,[19,82,89,90] PBE0 yields λ_{max} in very good agreement with experimental trends for the short-wavelength dyes, but the discrepancies significantly increase for the compounds with the smallest transition energies. Indeed, in the lower part of Table 1, it is PBE that yields the best estimates. For the 24 AQ, we obtain mean signed errors (MSE, experiment-theory) of 127, −71, 12, 67, 85, and 53 nm for HF, PBE, PBE0, LC-PBE, LC-ωPBE, and CAM-B3LYP, respectively. The corresponding mean absolute errors (MAE) amount to 127, 74, 19, 67, 85, and 53 nm, indicating that LR-DFT and HF systematically underestimate the λ_{max}. Consistently with the findings of ref 82, PBE0 is clearly closer to experiment, with a MAE less than half of the second competitor, namely CAM-B3LYP. However, the ordering of the compounds is also crucial for an efficient molecular design. Range-separated functionals provide the valid 1,4-OH > 1-NH$_2$ classification whereas PBE0 does not, but the reverse situation also appears (1,2-OH versus 1,8-OH), and cases can also be noted in Table 1 for which all approaches fail (2-OMe versus 1,2-OMe).

The situation differs in Table 2 where the spectra of AB derivatives are listed. Model and real-life AB have been considered, though we have not included OH substituents in the panel as such hydroxy-AB tend to undergo tautomerism that might impede straightforward theory/experiment comparisons. On the contrary, several push−pull molecules (4-NO$_2$, 4′-NH$_2$, and alike) having a strong charge-transfer character are tackled in Table 2. As for AQ, the methodological ordering of λ_{max} follows the amount of exact exchange at medium interelectronic distance. Nevertheless, CAM-B3LYP has now a slight edge over PBE0, and the accuracy difference between the λ_{max} obtained with global and range-separated approaches becomes less striking than for the AQ listed in Table 1. Indeed, we obtain MAE (MSE) of 64 (64) nm, 90 (−90) nm, 25 (−20) nm, 33 (33) nm, 46 (46) nm, and 20 (15) nm for HF, PBE, PBE0, LC-PBE, LC-ωPBE, and CAM-B3LYP, respectively. In fact CAM-B3LYP is particularly efficient for structures presenting a small λ_{max}, and the theory/experiment discrepancy tends to increase when going down the column. Note that for both AB having a λ_{max} > 500 nm, PBE0 is closer to the experimental reference than the three range-separated functionals: the description of charge-transfer dyes is not

Table 1. 9,10-Anthraquinone (AQ) Main Visible Transition, Obtained with the IEF-PCM-TD-X/6-311+G(2d,p)//
IEF-PCM-PBE0/6-311G(d,p) Approach[a]

subst	solvent	HF	PBE	PBE0	LC-PBE	LC-ωPBE	CAM-B3LYP	exp	ref
none	ethanol	250	377	321	280	271	294	322	4
2-Me	ethanol	252	380	324	282	272	296	324	4
1-Me	ethanol	259	399	339	291	280	306	331	4
2-Ome	ethanol	286	491	391	328	312	348	363	4
1,2-OMe	ethanol	279	482	386	323	307	341	374	4
1-Ome	ethanol	279	480	387	333	317	347	378	4
2-OH	ethanol	285	507	389	327	311	347	378	4
1-OH	ethanol	291	479	398	347	330	360	402	4
1,2,3-OH	ethanol	284	471	395	346	328	359	414	4
1,3-OH	ethanol	297	491	408	357	339	371	418	4,136
1,8-OH	ethanol	302	505	419	368	349	380	429	4
1,5-OH	ethanol	300	502	417	361	343	376	432	4
1,5-OH,3-Me	ethanol	299	498	415	360	342	374	433	137
1,2-OH	ethanol	299	524	426	359	340	376	435	4,136
1,3,8-OH,6-Me	ethanol	309	522	433	381	360	394	436	4
2-NH$_2$	ethanol	311	587	459	370	349	396	449	138
1,3,6,8-OH	ethanol	316	548	451	394	371	408	452	4
1-NH$_2$	ethanol	327	557	463	394	374	413	476	138
1,4-OH	ethanol	336	530	456	408	389	418	480	4
1,2,4-OH	ethanol	332	534	456	406	387	417	483	4
1,4,5-OH	ethanol	343	549	469	420	399	430	489	4
1,4,5,8-OH	ethanol	365	587	504	454	431	464	560	4
1,4-NH$_2$	ethanol	404	577	522	474	456	486	592	136
1,4-NHEt	ethanol	437	626	568	516	496	528	642	10

[a] PBE0 values are taken from ref 19. All values are in nm.

Table 2. λ_{max} (nm) of Azobenzenes (AB) Computed with the C-PCM-TD-X/6-311+G(2d,p)//C-PCM-PBE0/6-311G(d,p)
Scheme

subst/compound	solvent	HF	PBE	PBE0	LC-PBE	LC-ωPBE	CAM-B3LYP	exp	ref
none	EtOH	297	377	342	310	300	325	320	139
4-F	EtOH	295	381	345	313	302	326	320	139
4-Me	EtOH	301	388	350	316	306	331	323	139
4-Br	EtOH	300	403	355	316	305	332	325	139
4,4'-F	EtOH	294	386	347	315	304	328	325	139
4,4'-Br	EtOH	303	425	367	322	310	339	326	139
4-phenylazomaleinanil	CHCl$_3$	302	406	357	318	308	334	329	2
4,4'-Me	EtOH	304	396	357	322	311	337	330	139
4-OMe	EtOH	306	414	366	329	318	343	344	136,139
4,4'-OMe	EtOH	312	433	380	341	329	356	355	136,139
4-NH$_2$	MeOH	330	445	399	360	348	375	386	2
4,4'-NH$_2$	EtOH	342	475	422	377	363	394	399	136
4-NMe$_2$	MeOH	334	477	418	371	357	387	408	2
4-NHPh	EtOH	335	524	438	372	357	394	411	2
6'-OBu,2,6-NH$_2$,3,3'-azopdipyridine	MeOH	330	442	401	377	366	383	435	2
2'-NH$_2$-azobenzenenaphthalene	MeOH	376	496	451	411	397	427	439	2
4-NO$_2$, 4'-NH$_2$	50% EtOH	365	603	483	402	389	428	443	2
2,4-NH$_2$-azobenzenenaphthalene	EtOH	338	476	441	381	370	386	451	2
4-NO$_2$, 4'-N(Et)(CH$_2$CH$_2$CN)	MeOH	358	629	492	399	384	428	455	2
4-NO$_2$, 4'-NHPh	50% EtOH	363	700	527	408	392	442	483	2
4-NO$_2$, 4'-N(Et)(CH$_2$CH$_2$OH)	50% EtOH	369	662	513	415	399	443	503	2
4-NO$_2$, 2-Cl,4'-N(Et)(CH$_2$CH$_2$OH)	50% EtOH	372	666	525	425	410	467	517	2

systematically improved by inclusion of LR terms. Finally, the molecular ordering is generally correct although one noteworthy mismatch could be detected (6'-OBu,2,6-NH$_2$, 3,3'-azodipyridine versus 4,4'-NH$_2$): all approaches, but LC-ωPBE, disagree with experiments.

Table 3 summarizes our results for a 12 NQ set containing several 2,3-substituted structures that are known to be particularly problematic for global hybrids.[100] For these dyes, CAM-B3LYP outperforms PBE0, but the reverse is true for NQ with auxochroms at positions 5 and 8. One can also note

Table 3. First $\pi \rightarrow \pi^*$ Transition in 1,4-Naphthoquinone (NQ, C-PCM, Top) and Coumarins (CO, IEF-PCM, Bottom)[a]

subst	solvent	HF	PBE	PBE0	LC-PBE	LC-ωPBE	CAM-B3LYP	exp	ref
				1,4-Naphthoquinone					
2,3-Cl	methanol	258	412	349	296	283	316	337	140
2-OH	chcl$_3$	252	384	328	287	276	303	338	4,141
2,6-OH	ethanol	307	512	427	379	357	397	390	136
5-OMe	CHCl$_3$	281	521	411	350	330	368	396	4,141
2,3-Me,6-NH$_2$	cyclohexane	306	586	457	382	357	409	410	142
3,5-OH	CHCl$_3$	300	480	408	368	349	379	419	4,141
2,5-OH	CHCl$_3$	303	522	431	381	357	394	430	4,141
2,3-OH	CHCl$_3$	322	582	478	434	401	443	439	4,141
2-NHMe,3-Cl	cyclohexane	320	619	494	434	399	449	454	143
2-OMe,5,8-OH	CHCl$_3$	353	554	481	430	408	442	475	141
2-Cl,5,8-OH	CHCl$_3$	359	561	495	440	418	454	494	141
5-NH$_2$, 8-Ome	cyclohexane	361	599	515	464	438	479	564	142
				Coumarins					
4,7-OH (enol)	methanol	249	316	287	274	269	278	309	144
4-Me (enol)	ethanol	256	323	291	274	268	279	309	145,146
4-Me,7-OMe (enol)	water	260	340	303	285	278	290	322	147,148
4-Me,7-OH (enol)	water	261	337	303	284	277	288	323	147−150
7-OMe (enol)	water	266	341	306	290	283	295	324	151,152
4-Me,7-OH (cation)	water	274	374	330	307	301	312	345	147,149
4-Me,7-OMe (cation)	water	273	376	328	309	302	314	352	147
3-CN,7-OH (enol)	methanol	284	363	331	315	308	319	355	153
4-Me,7-OH (anion)	water	296	405	360	338	330	344	360	149,154,155
3-CN,7-OH (anion)	water	315	398	369	363	357	363	408	153

[a] All values are obtained through the PCM-TD-X/6-311+G(2d,p)//PCM-PBE0/6-311G(d,p) and are in nm. PBE0 values are from refs 99, 100, and 110 for NQ and CO, respectively.

Table 4. Diphenylamine (DPA, C-PCM, Top) and Diarylethenes (DA, IEF-PCM, Bottom) λ_{max} (nm), Obtained with the PCM-TD-X/6-311+G(2d,p)//PCM-PBE0/6-311G(d,p) Scheme[a]

					diphenylamine				
subst	solvent	HF	PBE	PBE0	LC-PBE	LC-ωPBE	CAM-B3LYP	exp	ref
none	hexane	248	320	284	273	265	280	286	156
4-NO$_2$	hexane	270	442	364	319	307	339	358	156−160
2,2′,4,4′-NO$_2$	ethanol	290−245	494−462	409−358	362−305	346−295	380−323	402−358	136,140,161
4,4′-NO$_2$	methanol	296	499	412	354	340	380	404	162
2,4′-NO$_2$	ethanol	296−258	532−455	434−364	370−310	352−300	397−331	407−353	161,163,164
2,4-NO$_2$	hexane	273−251	490−417	393−343	344−299	327−288	361−318	411−340	159
2-NO$_2$	hexane	289	497	416	364	346	384	415	156,158−160
2,2′-NO$_2$	hexane	286	509	417	362	343	383	420	158
2,6-NO$_2$	methanol	286	514	419	355	349	379	424	162

					diarylethenes				
R$_1$, R$_2$	solvent	HF	PBE	PBE0	LC-PBE	LC-ωPBE	CAM-B3LYP	exp.	ref
Cl, Cl	Hex	385	541	485	432	410	448	444	165,166
Cl, Ph	ACN	415	595	535	461	438	484	485	167
COOH,COOH	MeOH	440	700	599	509	477	537	531	165,166
Ph, Ph	Benz	456	687	605	507	479	537	531	165
COOEt,COOEt	ACN	429	670	578	496	465	520	540	167
p-Pyr., p-Pyr.	THF	468	744	636	525	494	559	551	168
CHO, CHO	Benz	471	791	670	563	522	592	580	165,166

[a] PBE0 figures are from refs 101 and 88 for DPA and DA, respectively.

systematic inversions (2,3-Cl versus 2-OH), but none of the proposed approach allows a λ_{max} classification clearly more appealing. Indeed, depending on the compounds, smaller (2,6-OH versus 5-OMe) or larger (2-NHMe,3-Cl versus 2-OMe,5,8-OH) proportion of exact exchange might help. Going from left to right in Table 3, we obtain MAE of 119,

99, 22, 42, 64, and 28 nm (the MSE are 119, −99, −11, 42, 64, and 26 nm). These values are in the line of the results obtained for AQ, although differences between PBE0 and CAM-B3LYP are strongly reduced for NQ.

The spectral data obtained for 10 neutral and charged CO are given in Table 3. The evaluation of the visible spectra

Table 5. Indigoids (IG) Main Visible Transition, Obtained with a IEF-PCM-TD-X/6-311+G(2d,p)//IEF-PCM-PBE0/6-311G(d,p) Scheme[a]

structure	subst	solvent	HF	PBE	PBE0	LC-PBE	LC-ωPBE	CAM-B3LYP	exp	ref
IG-a, X=X'=NH	none	CCl$_4$	400	651	572	519	490	525	594	169−172
	4,4'-Cl	CHCl$_3$	402	664	580	524	494	531	605	173,174
	4,4'-aza	EtOH	414	653	574	528	500	532	600	175
	5,5'-NO$_2$	TCE	383	637	550	503	475	507	580	176
	5,5'-Br	CHCl$_3$	407	708	599	534	502	542	611	173,174
	6,6'-NO$_2$	TCE	433	820	647	553	522	571	635	176
	6,6'-Br	TCE	399	636	569	519	490	524	588	176−178
	7,7'-Me	CHCl$_3$	406	671	586	527	498	534	612	174,179
	7,7'-aza	EtOH	370	624	539	490	461	494	556	175
X=X'=S	none	CHCl$_3$	354	655	544	465	428	483	546	180−187
	4,4'-Cl	benzene	356	646	546	467	431	484	548	188
	5,5'-NO$_2$	benzene	348	634	531	461	425	475	513	189
	5-OEt,5'-NO$_2$	benzene	367	841	603	487	447	512	562	190
	5-OEt,6'-NO$_2$	benzene	377	888	631	497	456	526	578	191
	6-NO$_2$	benzene	365	725	572	477	439	499	561	191
	7,7'-Br	benzene	353	663	546	464	428	481	546	192
X=X'=NMe	none	benzene	430	692	602	556	526	557	644	193
X=X'=O	none	CycloHex	292	524	430	379	358	386	413	194
X=X'=Se	none	benzene	354	647	568	471	433	496	562	195,196
X=NH, X'=S	none	benzene	376	657	556	488	456	501	574	197
IG-b	none	CHCl$_3$	339	560	494	448	415	454	505	185,186
IG-c	none	CHCl$_3$	327	529	456	418	387	424	458	185−187,198
IG-d	none	CHCl$_3$	323	550	472	427	392	434	467	187
IG-e	none	DMSO	324	438	395	366	353	374	413	134
IG-f	none	DMSO	346	582	490	438	415	446	516	134
IG-g	none	DMSO	329	556	444	371	357	391	455	134
IG-h, X=NH	none	DMSO	385	649	536	473	448	488	551	134
IG-h, X=S	none	Benzene	364	631	517	441	413	461	505	197
IG-i	none	DMSO	391	626	519	437	417	461	491	134
IG-j	none	methanol	256	368	325	298	290	305	355	199
IG-k	none	methanol	212	321	285	266	258	271	317	199

[a] More details can be found in refs 102−105.

of amino-CO is very challenging as both state-specific solvation and vibronic coupling could play a significant role.[112,113] Therefore, only hydroxy-CO are included in our set. As for the other dyes, HF (PBE) provides the smallest (largest) λ_{max} and hybrids stand in between, with wavelengths almost proportional to the exact exchange percentage at intermediate r_{12}. For CO, PBE, and PBE0 yield about the same accuracy but with opposite signed errors. Indeed the MSE are 67, −17, 20, 37, 43, and 33 nm for HF, PBE, PBE0, LC-PBE, LC-ωPBE, and CAM-B3LYP, respectively, while the MAE is equal to the MSE but for PBE (19 nm). All hybrids reproduce quite accurately the effect of protonation with predicted bathochromic shifts of 25 ± 2 nm to be compared to the experimental values of 22 (4-Me,7-OH−CO) and 30 nm (4-Me,7-OMe−CO). A basic medium modifies the λ_{max} of 3-CN,7-OH−CO by 53 nm, that is correctly reproduced by LC-PBE (48 nm) and LC-ωPBE (49 nm) but underestimated by HF (31 nm), PBE (35 nm), and PBE0 (38 nm). However, for 4-Me,7-OH CO, all hybrids exaggerate the impact of the enol-anion reaction.

Although DPA dyes show a significant charge-transfer character, global hybrids like PBE0 provide very accurate λ_{max} probably because the distance between the electron donor and the electron acceptor is rather small.[101] Table 4 confirms this conclusion with a MAE of 8 nm for

PBE0 but 27 nm for CAM-B3LYP (other schemes produce even larger average errors). Some DPA present two peaks, and the only drawback of PBE0 is that the separation between these two absorptions ($\Delta\lambda$) is 70 nm instead of 54 nm for 2,4'-NO$_2$-DPA but 50 nm instead of 71 nm for 2,4-NO$_2$-DPA. However, this problem cannot be corrected by LR-DFT nor PBE nor HF. For the DA of Table 4, that are characterized by a very delocalized first excited state,[123] we have the reverse situation with a large error with PBE0 (MAE=64 nm), whereas LR-DFT are closer to the experimental data, especially CAM-B3LYP that provides a MAE of 8 nm and a maximal discrepancy limited to 20 nm.

Table 5 lists the results for more than 30 dyes of the IG family. For thioindigo (X=X'=S) derivatives, the PBE0 functional has been found astonishingly efficient[104] but is less accurate for indigo (X=X'=NH) dyes for which B3LYP was more adequate.[103] In the indirubin/isoindigo series (IG-e-IG-i), no global hybrid functional gives the correct ordering of the compounds.[105] In the IG-a series, modifying only the X and X' atoms leads to the following λ_{max} ordering (in the nonpolar aprotic solvents used here): NMe,NMe > NH,-NH > NH,S > Se,Se > S,S > O,O. This order is not reproduced by HF (that predicts no difference between thio and selenoindigo), nor PBE (that incorrectly foresees a bigger

λ_{max} for sulfur than amine-based compounds) nor PBE0 (that reverses the order of X=X′=Se and X=NH, X′=S), but is correctly predicted by the three range-separated functionals, a significant chemical success. Of course, for these six structures, the PBE0 wavelengths are always much closer to experiment than LR-DFT. However, relative changes are also better reproduced by LR-DFT. For instance, the wavelength difference between the selenoindigo and oxy-indigo is 3.0 times larger than the $\Delta\lambda_{max}$ separating indigo and its N−Me form (149/50 nm). This ratio is exaggerated by PBE0 (4.6) but reasonably reproduced by LC-PBE (2.5), LC-ωPBE (2.4), and CAM-B3LYP (2.8). Concerning the substitution of the outer-phenyl rings, all hybrid schemes provide the correct ordering for thioindigo and indigo but for some cases in which the experimental data are extremely close (within 1 or 2 nm). In the Wille and Lüttke "linkage" series,[134] all IG-e - IG-i, HF, PBE, PBE0, and CAM-B3LYP invert IG-i and IG-f, whereas LC-PBE and LC-ωPBE predict almost equal absorption wavelengths for these two dyes, that is certainly a major improvement. A couple of thioindigo structures[104] for which PBE0 produces the largest errors (5-OEt,5′-NO$_2$ and 5-OEt,6′-NO$_2$) are overcorrected by LR-DFT, and even CAM-B3LYP undershoots their λ_{max} by about 50 nm, confirming that the description of charge-transfer excited states is not systematically improved by range-separated functionals. Overall, the MAE are 170, 96, 19, 70, 99, and 58 nm for HF, PBE, PBE0, LC-PBE, LC-ωPBE, and CAM-B3LYP, respectively. This confirms the superiority of PBE0 for absolute wavelength estimations although LR-DFT appears to be authorized to give more consistent chemical conclusions.

B. Statistical Treatment and Corrections. Statistical analysis for the three main families (AQ, AB, and IG) and the complete set of dyes are given in Table 6. A graphical comparison is plotted in Figure 4 for the LC-ωPBE functional. It is clear that HF (PBE) considerably undershoots (overestimates) the experimental λ_{max} by 116 and 87 nm on average. Hybrids perform significantly better for all dye subsets (but CO). While CAM-B3LYP yields the smallest MSE and MAE for AB and DA, PBE0 appears more efficient for the other five families. On average, for the full set (118 transitions), we obtain a MAE of 22 nm only with PBE0, whereas CAM-B3LYP produces almost twice this error. Nevertheless, the PBE0 maximal deviations remain unacceptably large: −74 and +90 nm. In the eV scale, the PBE0 MAE attains 0.14 eV and the RMS is 0.17 eV. As we have considered a very extended and diverse set of dyes, this value can be regarded as a new 'expected accuracy' for organic dye design with TD-DFT. It is worth comparing this performance with the 0.19 eV (37 nm) MAE obtained with B3LYP/6-31G by Guillaumont and Nakamura for a smaller set of dyes. The two other extended studies are due to Fabian who reported B3LYP/6-31+G(d) MAE of 0.29 and 0.24 eV for $\pi \rightarrow \pi^*$ transitions in sulfur-free and sulfur-bearing molecules, respectively.[17,135] The increased performance here reported mainly originates in the use of (much) more extended basis sets and the explicit consideration of solvent effects, that are essential for a realistic simulation of the experimental setups.

Table 6. Statistical Analysis for the AQ, AB, and IG Series[a]

family	method	without fit				with linear correction	
		MSE	MAE	RMS	R^2	MAE	RMS
AQ	HF	127	127	132	0.97	11	14
	PBE	−71	74	80	0.78	28	36
	PBE0	12	19	27	0.96	12	15
	LC-PBE	67	67	71	0.98	8	10
	LC-ωPBE	85	85	89	0.99	8	9
	CAM-B3LYP	53	33	58	0.98	8	10
AB	HF	64	64	75	0.89	15	21
	PBE	−90	90	103	0.83	22	27
	PBE0	−20	25	27	0.93	12	17
	LC-PBE	33	33	43	0.95	10	14
	LC-ωPBE	46	46	54	0.96	10	14
	CAM-B3LYP	15	20	28	0.94	10	16
IG	HF	170	170	174	0.89	19	26
	PBE	−96	96	116	0.71	34	42
	PBE0	6	19	23	0.93	17	21
	LC-PBE	70	70	72	0.97	10	13
	LC-ωPBE	99	99	101	0.97	12	14
	CAM-B3LYP	58	58	60	0.98	10	12
All	HF	116	116	127	0.76	37	45
	PBE	−86	87	102	0.81	30	40
	PBE0	−3	22	29	0.91	22	28
	LC-PBE	52	52	58	0.94	18	23
	LC-ωPBE	71	71	78	0.94	18	23
	CAM-B3LYP	37	38	46	0.93	20	25

[a] All include the complete data from Tables 1−5. All values (but R^2) are given in nm.
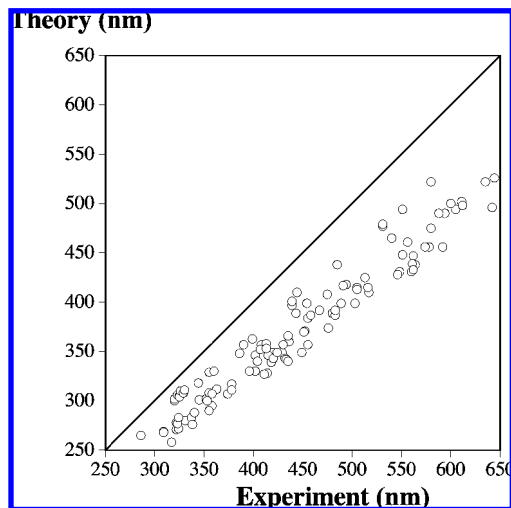

Figure 4. Comparison between the LC-ωPBE and measured λ_{max} (nm) for the full set of transitions. The central line indicates a perfect theory/experiment match.

To check the consistency between experimental and theoretical data, we have performed simple linear regressions on the different dye sets. Results are summarized in Table 6. HF and PBE obviously provide much smaller correlation coefficients than the hybrid approaches. Therefore, one can definitely discard HF and PBE for dye design: they provide not only the poorest absorption wavelength estimates but also the less consistent auxochromic displacements. Applying a linear correction to the PBE0 data is just useless, as the MAE
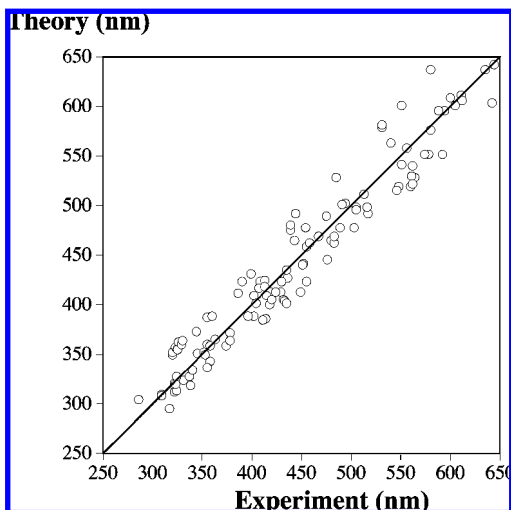
TD-DFT Performance for the Spectra of Organic Dyes

J. Chem. Theory Comput., Vol. 4, No. 1, 2008 **131**

Figure 5. Comparison between experimental λ_{max} and the values obtained by eq 3.

and RMS are almost unmodified. On the contrary, the R^2 obtained with the range-separated functionals is at least 0.93, confirming the interest of such approaches for classifying molecules according to their transition energies. Therefore, a linear correction improves the results of the three TD-LR-DFT schemes, especially for the two LC functionals. For instance, using

$$\lambda^{best} = -38.63 + 1.295 \times \lambda^{LC-\omega PBE} \qquad (3)$$

provides a MAE limited to 18 nm and a rms of 23 nm, that are at least three times smaller than the uncorrected LC-ωPBE data. Additionally, this MAE represents a 20% improvement over the (raw or fitted) PBE0 error. The impact of eq 3 is illustrated in Figure 5, and it is striking that the maximal deviations are now limited to +57 and −41 nm, both being smaller than the prior-to-fitting MAE. From Table 6, it is also striking that considering a single dye family and performing a calibration is extremely efficient as a better correlation coefficient and smaller average errors are systematically attained with range-separated functionals. Therefore, if one is able to establish a calibration curve for a given family of dye, the use of TD-LR-DFT should lead to the sufficient accuracy for the design of a new dye structure.

IV. Conclusions

Using TD-DFT, we have assessed the efficiency of several functionals for reproducing the experimental UV/vis $\pi \rightarrow \pi^*$ absorption wavelength of a set of 100+ organic dyes belonging to the classes of major industrial interest: azobenzenes, anthraquinones, indigos, diarylethenes, ... It was found that the computed λ_{max} systematically obey a PBE > PBE0 > CAM-B3LYP > LC-PBE > LC-ωPBE > HF order. This result can be rationalized by the total amount of exact exchange in each functional. Overall, PBE0 provides the smallest error with an average absolute deviation limited to 0.14 eV/22 nm. We state that this value should be regarded as a reference *expected PCM-TD-PBE0 accuracy* for low-lying excited states of conjugated organic compounds. The second best approach, CAM-B3LYP, suffers larger deviations (0.26 eV/38 nm) but appears particularly well suited

for studying dyes with a very delocalized excited state. On the contrary, HF and PBE give very poor estimates with average errors of 0.97 eV/116 nm and 0.45 eV/87 nm, respectively. If range-separated hybrids cannot beat PBE0 in terms of absolute λ_{max}, they provide more consistent evaluations of the auxochromic shifts. Indeed, linear fittings demonstrate that LR-functionals systematically give large R^2. Consequently, using a calibration equation such as eq 3 can considerably improve the accuracy of the LR computations. This is especially true when the statistical treatment is performed for a given dye family, for which average errors close to 10 nm are indeed obtained, allowing an efficient dye molecular design as it combines nearly quantitative wavelength estimates to chemically sound classifications. For the complete set of dyes, using scaled LR-DFT improves the PBE0 MAE by about 20%.

Of course, only low-lying π^* excited states of conjugated organic molecules have been considered in the present investigation. Care should be taken before applying eq 3 to other types of excitations or structures. However, for Rydberg states in small molecules it is clear that range-separated hybrids are adequate,[64,73,85] whereas these functionals are as accurate as global hybrids for $n \rightarrow \pi^*$ transitions.[88] Therefore, this contribution paves the way toward accurate, yet affordable, estimations of the excited-state energies of medium and large molecules. We are currently investigating inorganic structures to test the transferability of this approach.

References

(1) Griffiths, J. *Colour and Constitution of Organic Molecules;* Academic Press: London, 1976.

(2) Green, F. J. *The Sigma-Aldrich Handbook of Stains, Dyes and Indicators;* Aldrich Chemical Company, Inc.: Milwaukee, WI, 1990.

(3) Zollinger, H. *Color Chemistry, Syntheses, Properties and Applications of Organic Dyes and Pigments,* 3rd ed.; Wiley-VCH: Weinheim, Germany, 2003.

(4) Thomson, R. H. *Naturally Occurring Quinones,* 2nd ed.; Academic Press: London, U.K., 1971.

(5) Natansohn, A.; Rochon, P. *Chem. Rev.* **2002**, *102*, 4139−4176.

(6) Murakami, H.; Kawabuchi, A.; Kotoo, K.; Kunitake, M.; Nakashima, N. *J. Am. Chem. Soc.* **1997**, *119*, 7605−7606.

(7) Qu, D. H.; Wang, Q. C.; Ren, J.; Tian, H. *Org. Lett.* **2004**, *6*, 2085−2088.

(8) Fry, M.; Pudney, M. *Biochem. Pharmacol.* **1992**, *43*, 1545−1553.

(9) Cai, P.; Kong, F.; Ruppen, M.; Glasier, G.; Carter, G. *J. Nat. Prod.* **2005**, *68*, 1736−1742.

(10) Christie, R. M. *Colour Chemistry;* The Royal Society of Chemistry: Cambridge, U.K., 1991.

(11) Michaux, C.; Rolin, S.; Dogne, J.-M.; Durant, F.; Masereel, B.; Delarge, J.; Wouters, J. *Bioorg. Med. Chem. Lett.* **2001**, *11*, 1019−1022.

(12) Michaux, C.; Charlier, C.; Julemont, F.; de Leval, X.; Dogne, J. M.; Pirotte, B.; Durant, F. *Eur. J. Med. Chem.* **2005**, *40*, 1316−1324.

(13) Irie, M. *Chem. Rev.* **2000**, *100*, 1685−1716.

(14) Feringa, B. L. *Molecular Switches;* Wiley-VCH: Weinheim, Germany, 2001.

(15) Perrier, A.; Maurel, F.; Aubard, J. *J. Photochem. Photobiol. A: Chem.* **2007**, *189*, 167−176.

(16) Schäfer, A. *Modern Methods and Algorithms of Quantum Chemistry;* 2nd ed.; John von Neumann Institute for Computing: Jülich, Germany, 2000; Vol. 3 of *NIC*.

(17) Fabian, J. *Theor. Chem. Acc.* **2001**, *106*, 199−217.

(18) Jacquemin, D.; Perpete, E. A. *Chem. Phys. Lett.* **2006**, *429*, 147−152.

(19) Jacquemin, D.; Assfeld, X.; Preat, J.; Perpete, E. A. *Mol. Phys.* **2007**, *105*, 325−331.

(20) Perdew, J. P.; Ruzsinsky, A.; Tao, J.; Staroverov, V. N.; Scuseria, G. E.; Csonka, G. I. *J. Chem. Phys.* **2005**, *123*, 06 2001.

(21) Cossi, M.; Barone, V. *J. Chem. Phys.* **2001**, *115*, 4708−4717.

(22) Jacquemin, D.; Preat, J.; Wathelet, V.; André, J. M.; Perpete, E. A. *Chem. Phys. Lett.* **2005**, *405*, 429−433.

(23) Jacquemin, D.; Preat, J.; Perpete, E. A. *Chem. Phys. Lett.* **2005**, *410*, 254−259.

(24) Petit, L.; Quartarolo, A.; Adamo, C.; Russo, N. *J. Phys. Chem. B* **2006**, *110*, 2398−2404.

(25) Quartarolo, A. D.; Russo, N.; Sicilia, E. *Chem. Eur. J.* **2006**, *12*, 6797−6803.

(26) Petit, L.; Adamo, C.; Russo, N. *J. Phys. Chem. B* **2005**, *109*, 12214−12221.

(27) Quartarolo, A. D.; Russo, N.; Sicilia, E.; Lelj, F. *J. Chem. Theory Comput.* **2007**, *3*, 860−869.

(28) Becke, A. D. *J. Chem. Phys.* **1993**, *98*, 5648−5652.

(29) Stephens, P. J.; Devlin, F. J.; Chabalowski, C. F.; Frisch, M. J. *J. Phys. Chem.* **1994**, *98*, 11623−11627.

(30) Adamo, C.; Barone, V. *J. Chem. Phys.* **1998**, *108*, 664−675.

(31) Hamprecht, F. A.; Cohen, A. J.; Tozer, D. J.; Handy, N. C. *J. Chem. Phys.* **1998**, *109*, 6264−6271.

(32) Schmider, H. L.; Becke, A. D. *J. Chem. Phys.* **1998**, *108*, 9624−9631.

(33) Ernzerhof, M.; Scuseria, G. E. *J. Chem. Phys.* **1999**, *110*, 5029−5036.

(34) Adamo, C.; Barone, V. *J. Chem. Phys.* **1999**, *110*, 6158−6170.

(35) Hoe, W. M.; Cohen, A. J.; Handy, N. C. *Chem. Phys. Lett.* **2001**, *341*, 319−328.

(36) Boese, A. D.; Handy, N. C. *J. Chem. Phys.* **2002**, *116*, 9559−9569.

(37) Staroverov, V. N.; Scuseria, G. E.; Tao, J.; Perdew, J. P. *J. Chem. Phys.* **2003**, *119*, 12129−12137.

(38) Boese, A. D.; Martin, J. M. L. *J. Chem. Phys.* **2004**, *121*, 3405−3416.

(39) Xu, X.; Goddard, W. A., III *Proc. Natl. Acad. Sci. U.S.A.* **2004**, *101*, 2673−2677.

(40) Keal, T. W.; Tozer, D. J. *J. Chem. Phys.* **2005**, *123*, 121103.

(41) Paizs, B.; Suhai, S. *J. Comput. Chem.* **1998**, *19*, 575−584.

(42) Jacquemin, D.; André, J. M.; Perpete, E. A. *J. Chem. Phys.* **2004**, *121*, 4389−4396.

(43) Jacquemin, D.; Femenias, A.; Chermette, H.; Ciofini, I.; Adamo, C.; André, J. M.; Perpete, E. A. *J. Phys. Chem. A* **2006**, *110*, 5952−5959.

(44) Champagne, B.; Perpete, E. A.; van Gisbergen, S.; Baerends, E. J.; Snijders, J. G.; Soubra-Ghaoui, C.; Robins, K.; Kirtman, B. *J. Chem. Phys.* **1998**, *109*, 10489−10498.

(45) Champagne, B.; Perpete, E. A.; Jacquemin, D.; van Gisbergen, S.; Baerends, E.; Soubra-Ghaoui, C.; Robins, K.; Kirtman, B. *J. Phys. Chem. A* **2000**, *104*, 4755−4763.

(46) Guillaumont, D.; Nakamura, S. *Dyes Pigm.* **2000**, *46*, 85−92.

(47) Tozer, D. J. *J. Chem. Phys.* **2003**, *119*, 12697−12699.

(48) Dreuw, A.; Head-Gordon, M. *J. Am. Chem. Soc.* **2004**, *126*, 4007−4016.

(49) Magyar, R. J.; Tretiak, S. *J. Chem. Theory Comput.* **2007**, *3*, 976−987.

(50) Krieger, J. B.; Li, Y.; Iafrate, G. J. *Phys. Rev. A* **1992**, *45*, 101−126.

(51) Legrand, C.; Suraud, E.; Reinhard, P. G. *J. Phys. B* **2002**, *35*, 1115−1128.

(52) Ciofini, I.; Chermette, H.; Adamo, C. *Chem. Phys. Lett.* **2003**, *380*, 12−20.

(53) Vignale, G.; Kohn, W. *Phys. Rev. Lett.* **1996**, *77*, 2037−2040.

(54) van Faasen, M.; Boeij, P. L.; van Leeuwen, R.; Berger, J. A.; Snijders, J. G. *Phys. Rev. Lett.* **2002**, *88*, 186401.

(55) Antony, J.; Grimme, S. *Phys. Chem. Chem. Phys.* **2006**, *8*, 5287−5293.

(56) Alonso, J. A.; Mananes, A. *Theor. Chem. Acc.* **2007**, *117*, 467−472.

(57) Wang, D. Y.; Ye, Q.; Li, B. G.; Zhang, G. L. *Nat. Prod. Res.* **2003**, *17*, 365−368.

(58) Bulat, F. A.; Toro-Labbé, A.; Champagne, B.; Kirtman, B.; Yang, W. *J. Chem. Phys.* **2005**, *123*, 014319.

(59) Savin, A. In *Recent Developments and Applications of Modern Density Functional Theory*; Seminario, J. M., Ed.; Elsevier: Amsterdam, 1996; Chapter 9, pp 327−354.

(60) Leininger, T.; Stoll, H.; Werner, H. J.; Savin, A. *Chem. Phys. Lett.* **1997**, *275*, 151−160.

TD-DFT Performance for the Spectra of Organic Dyes

J. Chem. Theory Comput., Vol. 4, No. 1, 2008 **133**

(61) Iikura, H.; Tsuneda, T.; Yanai, T.; Hirao, K. *J. Chem. Phys.* **2001**, *115*, 3540−3544.

(62) Heyd, J.; Scuseria, G. E.; Ernzerhof, M. *J. Chem. Phys.* **2003**, *118*, 8207−8215; **2006**, *124*, 219906 (E).

(63) Toulouse, J.; Colonna, F.; Savin, A. *Phys. Rev. A* **2004**, *70*, 062505.

(64) Tawada, T.; Tsuneda, T.; Yanagisawa, S.; Yanai, T.; Hirao, K. *J. Chem. Phys.* **2004**, *120*, 8425−8433.

(65) Yanai, T.; Tew, D. P.; Handy, N. C. *Chem. Phys. Lett.* **2004**, *393*, 51−56.

(66) Yanai, T.; Harrison, R. J.; Handy, N. C. *Mol. Phys.* **2005**, *103*, 413−424.

(67) Kamiya, M.; Sekino, H.; Tsuneda, T.; Hirao, K. *J. Chem. Phys.* **2005**, *122*, 234111.

(68) Rudberg, E.; Salek, P.; Helgaker, T.; Agren, H. *J. Chem. Phys.* **2005**, *123*, 184108.

(69) Sato, T.; Tsuneda, T.; Hirao, K. *Mol. Phys.* **2005**, *103*, 1151−1164.

(70) Sato, T.; Tsuneda, T.; Hirao, K. *J. Chem. Phys.* **2005**, *123*, 104307.

(71) Baer, R.; Neuhauser, D. *Phys. Rev. Lett.* **2005**, *94*, 043002.

(72) Peach, M. J. G.; Helgaker, T.; Salek, P.; Keal, T. W.; Lutnaes, O. B.; Tozer, D. J.; Handy, N. C. *Phys. Chem. Chem. Phys.* **2006**, *8*, 558−562.

(73) Peach, M. J. G.; Cohen, A. J.; Tozer, D. J. *Phys. Chem. Chem. Phys.* **2006**, *8*, 4543−4549.

(74) Chiba, M.; Tsuneda, T.; Hirao, K. *J. Chem. Phys.* **2006**, *124*, 144106.

(75) Cai, Z. L.; Crossley, M. J.; Reimers, J. R.; Kobayashi, R.; Amos, R. D. *J. Phys. Chem. B* **2006**, *110*, 15624−15632.

(76) Kobayashi, R.; Amos, R. D. *Chem. Phys. Lett.* **2006**, *420*, 106−109.

(77) Vydrov, O. A.; Scuseria, G. E. *J. Chem. Phys.* **2006**, *125*, 234109.

(78) Vydrov, O. A.; Heyd, J.; Krukau, V.; Scuseria, G. E. *J. Chem. Phys.* **2006**, *125*, 074106.

(79) Vydrov, O. A.; Scuseria, G. E.; Perdew, J. P. *J. Chem. Phys.* **2007**, *126*, 154109.

(80) Sekino, H.; Maeda, Y.; Kamiya, M.; Hirao, K. *J. Chem. Phys.* **2007**, *126*, 014107.

(81) Chiba, M.; Tsuneda, T.; Hirao, K. *J. Chem. Phys.* **2007**, *126*, 034504.

(82) Jacquemin, D.; Perpete, E. A.; Scalmani, G.; Frisch, M. J.; Kobayashi, R.; Adamo, C. *J. Chem. Phys.* **2007**, *126*, 144105.

(83) Jacquemin, D.; Perpete, E. A.; Medved', M.; Scalmani, G.; Frisch, M. J.; Kobayashi, R.; Adamo, C. *J. Chem. Phys.* **2007**, *126*, 191108.

(84) Nguyen, K. A.; Day, P. N.; Pachter, R. *J. Chem. Phys.* **2007**, *126*, 094303.

(85) Livshits, E.; Baer, R. *Phys. Chem. Chem. Phys.* **2007**, *9*, 2932−2941.

(86) Fromager, E.; Toulouse, J.; Jensen, H. J. A. *J. Chem. Phys.* **2007**, *126*, 074111.

(87) Sekino, H.; Maeda, Y.; Kamiya, M. *Mol. Phys.* **2005**, *103*, 2183−2189.

(88) Jacquemin, D.; Perpete, E. A.; Vydrov, O. A.; Scuseria, G. E.; Adamo, C. *J. Chem. Phys.* **2007**, *127*, 094102.

(89) Jacquemin, D.; Preat, J.; Charlot, M.; Wathelet, V.; André, J. M.; Perpete, E. A. *J. Chem. Phys.* **2004**, *121*, 1736−1743.

(90) Perpete, E. A.; Wathelet, V.; Preat, J.; Lambert, C.; Jacquemin, D. *J. Chem. Theory Comput.* **2006**, *2*, 434−440.

(91) Shen, L.; Ji, H. F.; Zhang, H. Y. *J. Mol. Struct. (THEOCHEM)* **2006**, *758*, 221−224.

(92) Zhang, Q. M.; Gong, X. D.; Xiao, H. M.; Xu, X. J. *Acta Chim. Sin.* **2006**, *64*, 381−387.

(93) Jacquemin, D.; Wathelet, V.; Preat, J.; Perpete, E. A. *Spectrochim. Acta, Part A* **2007**, *67*, 334−341.

(94) Fliegl, H.; Köhn, A.; Hättig, C.; Ahlrichs, R. *J. Am. Chem. Soc.* **2003**, *125*, 9821−9827.

(95) Chen, P. C.; Chieh, Y. C.; Wu, J. C. *J. Mol. Struct. (THEOCHEM)* **2005**, *715*, 183−189.

(96) Liu, J. N. *J. Mol. Struct. (THEOCHEM)* **2005**, *730*, 151−154.

(97) Briquet, L.; Vercauteren, D. P.; Perpete, E. A.; Jacquemin, D. *Chem. Phys. Lett.* **2006**, *417*, 190−195.

(98) Briquet, L.; Vercauteren, D. P.; André, J. M.; Perpete, E. A.; Jacquemin, D. *Chem. Phys. Lett.* **2007**, *435*, 257−262.

(99) Jacquemin, D.; Preat, J.; Wathelet, V.; Perpete, E. A. *Chem. Phys.* **2006**, *328*, 324−332.

(100) Perpete, E. A.; Lambert, C.; Wathelet, V.; Preat, J.; Jacquemin, D. *Spectrochim. Acta, Part A* **2007**, *68*, 1326−1333.

(101) Jacquemin, D.; Bouhy, M.; Perpete, E. A. *J. Chem. Phys.* **2006**, *124*, 204321.

(102) Jacquemin, D.; Preat, J.; Wathelet, V.; Perpete, E. A. *J. Mol. Struct. (THEOCHEM)* **2005**, *731*, 67−72.

(103) Jacquemin, D.; Preat, J.; Wathelet, V.; Perpete, E. A. *J. Chem. Phys.* **2006**, *124*, 074104.

(104) Jacquemin, D.; Preat, J.; Wathelet, V.; Fontaine, M.; Perpete, E. A. *J. Am. Chem. Soc.* **2006**, *128*, 2072−2083.

(105) Perpete, E. A.; Preat, J.; André, J. M.; Jacquemin, D. *J. Phys. Chem. A* **2006**, *110*, 5629−5635.

(106) Cave, R. J.; Castner, E. W., Jr. *J. Phys. Chem. A* **2002**, *106*, 12117−12123.

(107) Cave, R. J.; Burke, K.; Castner, E. W., Jr. *J. Phys. Chem. A* **2002**, *106*, 9294−9305.

(108) Preat, J.; Jacquemin, D.; Perpete, E. A. *Chem. Phys. Lett.* **2005**, *415*, 20−24.

(109) Preat, J.; Jacquemin, D.; Wathelet, V.; André, J. M.; Perpete, E. A. *J. Phys. Chem. A* **2006**, *110*, 8144−8150.

(110) Jacquemin, D.; Perpete, E. A.; Scalmani, G.; Frisch, M. J.; Assfeld, X.; Ciofini, I.; Adamo, C. *J. Chem. Phys.* **2006**, *125*, 164324.

(111) Santoro, F.; Improta, R.; Lami, A.; Bloino, J.; Barone, V. *J. Chem. Phys.* **2007**, *126*, 084509.

(112) Improta, R.; Barone, V.; Scalmani, G.; Frisch, M. J. *J. Chem. Phys.* **2006**, *125*, 054103.

(113) Improta, R.; Barone, V.; Santoro, F. *Angew. Chem., Int. Ed.* **2007**, *46*, 405−408.

(114) Majumdar, D.; Lee, H. M.; Kim, J.; Kim, K. S.; Mhin, B. J. *J. Chem. Phys.* **1999**, *111*, 5866−5872.

(115) Kobatake, S.; Morimoto, M.; Asano, Y.; Murakami, A.; Nakamura, S.; Irie, M. *Chem. Lett.* **2002**, 1224−1225.

(116) Goldberg, A.; Murakami, A.; Kanda, K.; Kobayashi, T.; Nakamura, S.; Ucjida, K.; Sekiya, H.; Fukaminato, T.; Kawau, T.; Kobatake, S.; Irie, M. *J. Phys. Chem. A* **2003**, *107*, 4982−4988.

(117) Giraud, M.; Léaustic, A.; Charlot, M. F.; Yu, P.; Césario, M.; Philouze, C.; Pansu, R.; Nakatani, K.; Ishow, E. *New. J. Chem.* **2005**, *29*, 439−446.

(118) Higashiguchi, K.; Matsuda, K.; Asano, A.; Murakami, A.; Nakamura, S.; Irie, M. *Eur. J. Org. Chem.* **2005**, 91−97.

(119) Clark, A. E. *J. Phys. Chem. A* **2006**, *110*, 3790−3796.

(120) Chen, D. Z.; Wang, Z.; Zhao, X. *J. Mol. Struct. (THEOCHEM)* **2006**, *774*, 77−81.

(121) Yokojima, S.; Matsuda, K.; Irie, M.; Murakami, A.; Kobayashi, T.; Nakamura, S. *J. Phys. Chem. A* **2006**, *110*, 8137−8143.

(122) Perpete, E. A.; Jacquemin, D. *J. Photochem. Photobiol. A: Chem.* **2007**, *187*, 40−44.

(123) Perpete, E. A.; Maurel, D.; Jacquemin, D. *J. Phys. Chem. A* **2007**, *111*, 5528−5535.

(124) Perdew, J. P.; Burke, K.; Ernzerhof, M. *Phys. Rev. Lett.* **1996**, *77*, 3865−3868.

(125) Heyd, J.; Scuseria, G. E. *J. Chem. Phys.* **2004**, *120*, 7274−7280.

(126) Song, J. W.; Hirosawa, T.; Tsuneda, T.; Hirao, K. *J. Chem. Phys.* **2007**, *126*, 154105.

(127) Frisch, M. J.; Trucks, G. W.; Schlegel, H. B.; Scuseria, G. E.; Robb, M. A.; Cheeseman, J. R.; Montgomery, J. A., Jr.; Vreven, T.; Kudin, K. N.; Burant, J. C.; Millam, J. M.; Iyengar, S. S.; Tomasi, J.; Barone, V.; Mennucci, B.; Cossi, M.; Scalmani, G.; Rega, N.; Petersson, G. A.; Nakatsuji, H.; Hada, M.; Ehara, M.; Toyota, K.; Fukuda, R.; Hasegawa, J.; Ishida, M.; Nakajima, T.; Honda, Y.; Kitao, O.; Nakai, H.; Klene, M.; Li, X.; Knox, J. E.; Hratchian, H. P.; Cross, J. B.; Bakken, V.; Adamo, C.; Jaramillo, J.; Gomperts, R.; Stratmann, R. E.; Yazyev, O.; Austin, A. J.; Cammi, R.; Pomelli, C.; Ochterski, J. W.; Ayala, P. Y.; Morokuma, K.; Voth, G. A.; Salvador, P.; Dannenberg, J. J.; Zakrzewski, V. G.; Dapprich, S.; Daniels, A. D.; Strain, M. C.; Farkas, O.; Malick, D. K.; Rabuck, A. D.; Raghavachari, K.; Foresman, J. B.; Ortiz, J. V.; Cui, Q.; Baboul, A. G.; Clifford, S.; Cioslowski, J.; Stefanov, B. B.; Liu, G.; Liashenko, A.; Piskorz, P.; Komaromi, I.; Martin, R. L.; Fox, D. J.; Keith, T.; Al-Laham, M. A.; Peng, C. Y.; Nanayakkara, A.; Challacombe, M.; Gill, P. M. W.; Johnson, B.; Chen, W.; Wong, M. W.; Gonzalez, C.; Pople, J. A. *Gaussian 03, Revision C.02;* Gaussian, Inc.: Wallingford, CT, 2004.

(128) Frisch, M. J.; Trucks, G. W.; Schlegel, H. B.; Scuseria, G. E.; Robb, M. A.; Cheeseman, J. R.; Montgomery, J. A., Jr.; Vreven, T.; Scalmani, G.; Kudin, K. N.; Iyengar, S. S.; Tomasi, J.; Barone, V.; Mennucci, B.; Cossi, M.; Rega, N.; Petersson, G. A.; Nakatsuji, H.; Hada, M.; Ehara, M.; Toyota, K.; Fukuda, R.; Hasegawa, J.; Ishida, M.; Nakajima, T.; Honda, Y.; Kitao, O.; Nakai, H.; Li, X.; Hratchian, H. P.; Peralta, J. E.; Izmaylov, A. F.; Brothers, E.; Staroverov, V.; Kobayashi, R.; Normand, J.; Burant, J. C.; Millam, J. M.; Klene, M.; Knox, J. E.; Cross, J. B.; Bakken, V.; Adamo, C.; Jaramillo, J.; Gomperts, R.; Stratmann, R. E.; Yazyev, O.; Austin, A. J.; Cammi, R.; Pomelli, C.; Ochterski, J. W.; Ayala, P. Y.; Morokuma, K.; Voth, G. A.; Salvador, P.; Dannenberg, J. J.; Zakrzewski, V. G.; Dapprich, S.; Daniels, A. D.; Strain, M. C.; Farkas, O.; Malick, D. K.; Rabuck, A. D.; Raghavachari, K.; Foresman, J. B.; Ortiz, J. V.; Cui, Q.; Baboul, A. G.; Clifford, S.; Cioslowski, J.; Stefanov, B. B.; Liu, G.; Liashenko, A.; Piskorz, P.; Komaromi, I.; Martin, R. L.; Fox, D. J.; Keith, T.; Al-Laham, M. A.; Peng, C. Y.; Nanayakkara, A.; Challacombe, M.; Chen, W.; Wong, M. W.; Pople, J. A. *Gaussian DVP, Revision C.01*; Gaussian, Inc.: Wallingford, CT, 2006.

(129) Stratmann, R. E.; Scuseria, G. E.; Frisch, M. J. *J. Chem. Phys.* **1998**, *109*, 8218−8224.

(130) Adamo, C.; Scuseria, G. E.; Barone, V. *J. Chem. Phys.* **1999**, *111*, 2889−2899.

(131) Curtiss, L. A.; Raghavachari, K.; Referm, P. C.; Pople, J. A. *Chem. Phys. Lett.* **1997**, *270*, 419−426.

(132) Barone, V.; Adamo, C. *J. Chem. Phys.* **1996**, *105*, 11007−11019.

(133) Tomasi, J.; Mennucci, B.; Cammi, R. *Chem. Rev.* **2005**, *105*, 2999−3094.

(134) Wille, E.; Lüttke, W. *Chem. Ber.* **1973**, *106*, 3240−3257.

(135) Fabian, J.; Diaz, L. A.; Seifert, G.; Niehaus, T. *J. Mol. Struct. (THEOCHEM)* **2002**, 594, 41−53.

(136) Weast, R. C. *Handbook of Chemistry and Physics,* 51st ed.; The Chemical Rubber Company: Cleveland, OH, 1970.

(137) Günaydin, K.; Topcu, G.; Ion, R. M. *Nat. Prod. Lett.* **2002**, *16*, 65−70.

(138) Fabian, J.; Nepras, M. *Collect. Czech. Chem. Commun.* **1980**, 45, 2605−2620.

(139) Gore, P. H.; Wheeler, O. H. *J. Org. Chem.* **1961**, *26*, 3295−3298.

(140) Grasselli, J. G. *Atlas of Spectral Data and Physical Constants for Organic Compounds;* The Chemical Rubber Company: Cleveland, OH, 1973.

(141) Singh, I.; Ogata, R. T.; Moore, R. E.; Chang, C. W. J.; Scheuer, P. J. *Tetrahedron* **1968**, *24*, 6053−6073.

(142) Chu, K. Y.; Griffiths, J. *J. Chem. Res.* **1978**, 180−181.

(143) Chu, K. Y.; Griffiths, J. *J. Chem. Soc., Perkin Trans. I* **1978**, 1083−1087.

(144) Wolfbeis, O. S.; Uray, G. *Monat. Chem.* **1978**, *109*, 123−136.

(145) Ganguly, B. K.; Bagchi, P. *J. Org. Chem.* **1956**, *21*, 1415−1419.

(146) Wheelcock, C. E. *J. Am. Chem. Soc.* **1959**, *81*, 1348−1352.

(147) Yakatan, G. J.; Juneau, R. J.; Schulman, S. G. *Anal. Chem.* **1972**, *44*, 1044−1046.

(148) Giri, R.; Rathi, S. S.; Machwe, M. K.; Murti, V. V. S. *Spectrochim. Acta, Part A* **1988**, *44*, 805−807.

(149) Moriya, T. *Bull. Chem. Soc. Jpn.* **1988**, *61*, 1873−1886.

(150) Kumar, S.; Rao, V. C.; Rastogi, R. C. *Spectrochim. Acta, Part A* **2001**, *57*, 41−47.

(151) Heldt, J. R.; Helds, J.; Ston, M.; Diehl, H. A. *Spectrochim. Acta, Part A* **1995**, *51*, 1549−1563.

(152) Azuma, K.; Suzuki, S.; Uchiyama, S.; Kajiro, T.; Santa, T.; Imai, K. *Photochem. Photobiol. Sci.* **2003**, *2*, 443−449.

(153) Wolfbeis, O. S. *Z. Naturforsch., Teil A* **1977**, *32A*, 1065−1067.

(154) Sherman, W. R. *Anal. Chem.* **1968**, *40*, 803−805.

(155) Sun, W. C.; Gee, K. R.; Haugland, R. P. *Bioorg. Med Chem. Lett.* **1998**, *8*, 3107−3110.

(156) Lutskii, A. E.; Konel'skaya, V. N. *Z. Obs. Khim.* **1960**, *30*, 3773−3782.

(157) Bugai, P. M.; Konel'skaya, V. N. *Izv. Akad. Nauk. SSSR - Ser. Fiz.* **1954**, *18*, 695−697.

(158) Bugai, P. M.; Konel'skaya, V. N.; Gol'berkova, A. S.; Bazhenova, L. M. *Z. Fiz. Khim.* **1962**, *36*, 2233−2234.

(159) Bell, M. G. W.; Day, M.; Peters, A. T. *J. Soc. Dyers Colour.* **1966**, *82*, 410−414.

(160) Day, M.; Peters, A. T. *J. Soc. Dyers Colour.* **1969**, *85*, 8−13.

(161) Schroeder, W. A.; Wilcox, P. E.; Trueblood, K. N.; Dekker, A. O. *Anal. Chem.* **1951**, *23*, 1740−1747.

(162) Csaszar, J. *Acta Phys. Chem.: (Szeged)* **1987**, *33*, 11−21.

(163) Asquith, R. S.; Bridgeman, I.; Peters, A. T. *J. Soc. Dyers Colour.* **1965**, *81*, 439−441.

(164) Asquith, R. S.; Peters, A. T.; Wallace, F. *J. Soc. Dyers Colour.* **1968**, *84*, 507−510.

(165) Lucas, L. N. Dithienylcyclopentene Optical Switches: Towards Photoresponsive Supramolecular Materials, Ph.D. thesis, Rijksuniversiteit Groningen: 2001.

(166) Lucas, L. N.; de Jong, J. J.; van Esch, J. H.; Kellogg, R. M.; Feringa, B. L. *Eur. J. Org. Chem.* **2003**, 155−166.

(167) Browne, W. R.; de Jong, J. J.; Kudernac, T.; Walko, M.; Lucas, L. N.; Uchida, K.; van Esch, J. H.; Feringa, B. L. *Chem. Eur. J.* **2005**, *11*, 6430−6441.

(168) Qin, B.; Yao, R.; Zhao, X.; Tian, H. *Org. Biolmol. Chem.* **2003**, *1*, 2187−2191.

(169) Sheppard, S. E.; Newsome, P. T. *J. Am. Chem. Soc.* **1942**, *64*, 2937−3946.

(170) Klessinger, M.; Lüttke, W. *Tetrahedron* **1963**, 19 Suppl. 2, 315−335.

(171) Klessinger, M.; Lüttke, W. *Chem. Ber.* **1966**, *99*, 2136−2145.

(172) Monahan, A. R.; Kuder, J. E. *J. Org. Chem.* **1972**, *37*, 4182−4184.

(173) Brode, W. R.; Pearson, E. G.; Wyman, G. M. *J. Am. Chem. Soc.* **1954**, *76*, 1034−1036.

(174) Weinstein, J.; Wyman, G. M. *J. Am. Chem. Soc.* **1956**, *78*, 2387−2390.

(175) Lüttke, W.; Hunsdiecker, D. *Chem. Ber.* **1966**, *99*, 2146−2154.

(176) Saddler, P. W. *J. Org. Chem.* **1956**, *21*, 316−318.

(177) Friedländer, P.; Bruckner, S.; Deutsch, G. *J. Liebigs Ann. Chem.* **1912**, *388*, 23−49.

(178) Ettinger, L.; Friedländer, P. A. *Ber. Dtsch. Chem. Ges.* **1912**, *45*, 2074−2080.

(179) Travasso, M. I. G.; Santos, P. C. S.; Oliveira-Campos, A. M. F.; Raposo, M. M. M.; Prasitpan, N. *Adv. Colour Sci. Technol.* **2003**, *6*, 95−99.

(180) Friedländer, P. *Ber. Dtsch. Chem. Ges.* **1908**, *41*, 772−777.

(181) Wyman, G. M.; Brode, W. R. *J. Am. Chem. Soc.* **1951**, *73*, 1487−1493.

(182) Brode, W. R.; Wyman, G. M. *J. Am. Chem. Soc.* **1951**, *73*, 4267−4270.

(183) Pummerer, R.; Marondel, G. *Chem. Ber.* **1960**, *99*, 2834−2839.

(184) Mostoslavskii, M. A.; Izmail'ski, V.; Shapkina, M. M. *J. Gen. Chem. USSR* **1962**, 32, 1731−1739.

(185) Lüttke, W.; Hermann, H.; Klessinger, M. *Angew. Chem., Int. Ed. Engl.* **1966**, *5*, 598−599.

(186) Hermann, H.; Lüttke, W. *Chem. Ber.* **1968**, *101*, 1715−1728.

(187) Luhmann, U.; Wentz, F. G.; Knieriem, B.; Lüttke, W. *Chem. Ber.* **1978**, *111*, 3233−3245.

(188) Kirsch, A. D.; Wyman, G. M. *J. Phys. Chem.* **1977**, *81*, 413−420.

(189) Dokunikhin, N. S.; Gerasimenko, Y. E. *J. Gen. Chem. USSR* **1960**, *30*, 655−658.

(190) Dokunikhin, N. S.; Gerasimenko, Y. E. *J. Gen. Chem. USSR* **1960**, *30*, 1966−1968.

(191) Dokunikhin, N. S.; Gerasimenko, Y. E. *J. Gen. Chem. USSR* **1961**, *31*, 205−208.

(192) Dokunikhin, N. S.; Gerasimenko, Y. E. *J. Gen. Chem. USSR* **1960**, *30*, 1253−1255.

(193) Giuliano, C. R.; Hess, L. D.; Margerum, J. D. *J. Am. Chem. Soc.* **1968**, *90*, 587−594.

(194) Gusten, H. *Chem. Commun.* **1969**, 133−134.

(195) Fitjer, L.; Lüttke, W. *Chem. Ber.* **1972**, *105*, 919−928.

(196) Wyman, G. M.; Zarnegar, B. *J. Phys. Chem.* **1973**, *73*, 831−837.

(197) Haucke, G.; Paetzold, R. *Nova Acta Leopold. Suppl.* **1978**, *11*, 1−123.

(198) Gerken, R.; Fitjer, L.; Müller, P.; Usón, I.; Kowski, K.; Rademacher, P. *Tetrahedron* **1999**, *55*, 14429−14434.

(199) Junek, H.; Fischer-Colbrie, H.; Sterk, H. *Chem. Ber.* **1977**, *110*, 2276−2285.